SURFACE CHARACTERISTICS OF ROLL WAVES ON FREE FALLING FILMS

T. D. KARAPANTSIOS and A. J. KARABELAS

Chemical Process Engineering Research Institute and Chemical Engineering Department,
University of Thessaloniki, 540 06 Thessaloniki, Greece

Abstract—The focus of the present study is to identify and describe the surface waves on films running down a vertical wall, by applying a novel approach in which the time-dependent wave characteristics are not used explicitly. Using time records of film thickness at a station, a "spatial evolution portrait" of a surface wave is obtained by plotting the rate of displacement vs local film thickness. A specific, shell-like, pattern is easily recognized in all these portraits and it is representative of large (roll) waves, independent of film Reynolds number in the range Re = 500 to 13000. This type of representation is helpful in determining the salient features of roll waves and possibly for modeling the form of wavy interfaces. Calculations of the Eulerian surface accelerations provide additional evidence on the development of surface waves. Several statistical quantities of both the rate of displacement and Eulerian acceleration (i.e. maxima, minima, skewness etc.), have been calculated to provide more information on the character of surface motion. Assuming that roll waves travel with a constant phase velocity, the surface slopes are calculated at various Re. All slopes are smaller than $\approx 20°$, being steeper at the wave front than at the wave back. Interestingly, it appears that surface slopes are almost independent of film Re.

Key Words: falling film, roll waves, surface displacement, surface acceleration

1. INTRODUCTION

Free falling films are encountered in common industrial process equipment, where heat and mass transfer take place. A significant amount of research work—both experimental and theoretical—carried out over the last few decades, suggests that the performance of this equipment is influenced by the film characteristics and especially by the waviness at the gas/liquid interface. Indeed, the waves affect the transfer rates not only across the gas/liquid interface (e.g. Henstock & Hanratty 1979; McCready & Hanratty 1985) but also across the solid/liquid boundary (e.g. Brauner & Maron 1982). It is clear, therefore, that in order to model transport processes, the characteristics of the wavy interface and of the velocity field within the film must be known.

Many theoretical attempts have been made to describe the waves formed on free falling liquid films. The two general approaches are either flow stability analyses based on the Orr-Sommerfeld equation (e.g. Benjamin 1957), or analyses of nonlinear wave motion at *low Reynolds numbers (Re)* using integral forms of the momentum equation, following Kapitsa's (1964) approach. The recent work of Alekseenko *et al.* (1985) extends the study of nonlinear nonstationary waves to somewhat higher Re—still below 100.

In other relevant studies, Benney (1966), Lin (1974) and Nakaya (1975) performed nonlinear analyses, assuming one-dimensional waves, and derived a single equation (postulating "monochromatic" waves) which was found to hold fairly accurately at low Re. Pumir *et al.* (1983) solved this equation numerically in their study of solitary waves. Chang (1987), using dynamic singularity theory, derived closed-form solutions for the evolution of finite amplitude waves. It is important to point out that all the above studies are restricted to small Re, i.e. to Re values much lower than those usually encountered in practical applications.

Finite element solutions of the Navier–Stokes equations have been used very recently to study wave development from initial perturbations on the smooth film (Bach & Villadsen 1984; Kheshgi & Scriven 1987). In the former study stationary wave profiles are obtained. In the latter the flow is specified to be spatially periodic and fully developed conditions are obtained, i.e. waves of finite amplitude. Only some of the results from these important studies are in agreement with experimental observations, and their applicability is restricted to small Re. In particular, there is concern that the waveforms obtained are not in agreement with those measured.

Experimental studies on free falling films have shed considerable light on the problem but many questions still remain unresolved. The waves seem to grow from initial perturbations of film thickness which may occur at random time intervals. In some cases two-dimensional regular wave trains are observed—mostly at low Re and near the wave inception line. In other cases the waves are three-dimensional, irregular or of a form far from sinusoidal. Moreover, at relatively high Re, fast-moving large waves tend to overtake the small (capillary) waves, resulting in a complicated wave structure that appears to be of a *random* character. Consequently, in experimental studies the time records of film thickness are statistically analyzed (Chu & Dukler 1974, 1975; Takahama & Kato 1980; Karapantsios *et al.* 1989) with no reference to two- or three-dimensional, stationary or nonstationary, waves.

The above studies have shown that there are at least two classes of waves, i.e. large inertia-gravity waves (also known as "roll waves") and small waves in which interfacial tension may be significant together with other forces. Moreover, the available experimental data suggest that (under constant conditions) the roll waves travel with an almost constant celerity and that they can be relatively easily identified over a wide range of Re.

A modeling effort for the realistic description of *roll* wave structure was first undertaken by Maron *et al.* (1985). Recently, Brauner (1987) presented an extension of the model by taking into account the effect of turbulence. This rather complex model is based on different physical mechanisms controlling various zones along a roll wave. An essential input in this model is the *shape* of the roll wave surface. For simplification it is assumed that the surface at both the front and the back of the roll waves is linear. The recent numerical study of the velocity distribution within a roll wave by Wasden & Dukler (1989) also requires as an input the shape of the free surface.

Aside from the above deterministic modeling efforts, the shape of the interface is also required in studies in which the random character of the film surface is taken into account. An example of this approach is the recent study by Back & McCready (1988) in which local velocity gradients at the interface are computed (from reconstructions of the interface shape) by taking the inverse Fourier transform of the respective wave amplitude spectra.

Although some significant experimental data on falling film characteristics are included in the papers by Chu & Dukler (1974, 1975), Zabaras (1985) and others, it is felt that additional effort is required to describe the wave *surface* characteristics. Of particular interest is the reliable description of roll waves, which should aid significantly the aforementioned modeling efforts. This paper is considered a contribution in that direction. Data obtained in our laboratory (Karapantsios *et al.* 1989), for falling films inside a 50 mm i.d. pipe, are employed to study the surface characteristics of waves. The Re range covered is between Re ≈ 500 and Re ≈ 13000. In the next two sections of the paper the method of data interpretation is discussed and preliminary observations regarding interface shape, wave phase velocity and surface slopes are presented. In the following section the wave properties are examined by plotting the rate of surface displacement dh/dt vs the corresponding film thickness h. Data on surface acceleration d^2h/dt^2 are also presented and discussed in that section. Finally, statistical analysis of dh/dt and d^2h/dt^2 data is helpful in drawing physically significant conclusions about the falling film surface.

2. METHOD OF DATA INTERPRETATION

In this paper we analyze data on first and second time derivatives of the surface elevation, in order to gain new insight, i.e. beyond that afforded by the usual statistical analysis of film thickness traces $h(t)$. To some extent, the motivation for this approach is due to the recent work of coastal engineers and oceanographers who employ time derivatives of $h(t)$ to study waves on the sea surface. In this section the basic quantities are defined and their use in the above studies is outlined along with some typical results.

Let $h(t)$ be a time series of liquid film level, measured at a fixed station on a vertical wall. Assuming waves of permanent form, the time derivative of this signal (dh/dt) is related to the slope of the film surface (dh/dx) by the equation

$$\frac{dh}{dt} = C\frac{dh}{dx},$$ [1]

where C is the phase velocity of the waves, $dh/dx = \tan\alpha$, and α is the angle of inclination of the surface to the vertical.

If the sampling frequency of $h(t)$ is large enough then the time interval between successive measurements is very small. For the measurements by Karapantsios et al. (1989), the sampling frequency was 500 Hz and the corresponding time interval $\Delta t = 2$ ms. It can be further considered that this time interval $\Delta t = t_2 - t_1 = (t + \Delta t/2) - (t - \Delta t/2)$ is small enough so that the change in $h(t)$, $\Delta h = h_2 - h_1 = h(t + \Delta t/2) - h(t - \Delta t/2)$ is approximately linear. This, in turn, leads directly to the correspondence between $\bar{h} = (h_1 + h_2)/2$ and $t = t_1 + \Delta t/2$. For such small Δt (0.002 s), [1] can be approximated by

$$\frac{\Delta h}{\Delta t} = C\frac{\Delta h}{\Delta x}.$$

[2]

To avoid data misinterpretation Glazman (1986) suggests caution when first and second time derivatives are computed from film traces $h(t)$. His comments, which are very relevant to this study, are outlined here.

For the time series $h(t)$ one can calculate the time-averaged values $\bar{h}(t)$ within $\Delta t = 0.002$ s, as follows:

$$\bar{h}(t) = \frac{1}{\Delta t}\int_{t-\frac{\Delta t}{2}}^{t+\frac{\Delta t}{2}} h(t)\,dt \approx \frac{h_2 + h_1}{2}.$$

[3]

Then, the derivative of such an averaged signal is

$$\frac{\partial\bar{h}}{\partial t} = \frac{1}{\Delta t}\left[h\left(t + \frac{\Delta t}{2}\right) - h\left(t - \frac{\Delta t}{2}\right)\right]$$

[4]

and corresponds to $\bar{h}(t)$. Moreover, the second derivative can be computed by the formula

$$\frac{\partial}{\partial t}\left(\frac{\partial\bar{h}}{\partial t}\right) = \frac{\partial^2\bar{h}}{\partial t^2} = \left(\frac{1}{\Delta t}\right)\left[\left(\frac{\partial\bar{h}}{\partial t}\right)_{t+(\Delta t/2)} - \left(\frac{\partial\bar{h}}{\partial t}\right)_{t-(\Delta t/2)}\right]$$

$$= \left(\frac{1}{\Delta t}\right)^2 [h(t + \Delta t) - 2h(t) + h(t - \Delta t)]$$

and not by

$$\frac{\partial}{\partial t}\left(\frac{\partial\bar{h}}{\partial t}\right) = \left(\frac{1}{\Delta t}\right)\left[\left(\frac{\partial h}{\partial t}\right)_{t+(\Delta t/2)} - \left(\frac{\partial h}{\partial t}\right)_{t-(\Delta t/2)}\right].$$

[6]

Clearly [6] involves derivatives of the nonaveraged signal which "carry information about the variations of the (unfiltered) process $h(t)$ over an infinitesimal time interval". In the words of Glazman (1986), by applying [5] we "explicitly introduce a (temporal) yardstick and discard all oscillations with time scales under Δt".

The time derivatives of surface displacement are often used by researchers in the field of coastal and ocean engineering to describe the wavy sea surface. Their major interest is to understand the physical mechanisms controlling air–sea exchange processes, such as momentum, heat and mass transfer (e.g. Longuet-Higgins & Smith 1983).

Thorpe & Humphries (1980) suggested that there is a causal relationship between the "breaking" of waves and the rate of surface displacement dh/dt. Later, Longuet-Higgins & Smith (1983) employed a surface jump meter to determine the frequency of occurrence of breaking waves. They also proposed as a breaking criterion the condition

$$\left(\frac{dh}{dx}\right) > \left(\frac{dh}{dx}\right)_{max},$$

where $(dh/dx)_{max}$ was obtained from the theoretical work by Longuet-Higgins & Fox (1977). For a regular progressive gravity wave, the maximum inclination of the surface was calculated to be $30.37°$, or $(dh/dx)_{max} = \tan(30.37) = 0.58$. In order to evaluate (dh/dx) for each wave, these authors employed equation (1) with C an average phase velocity of the waves in the sampled record. Xu et al. (1986) attempted an improvement by computing a different phase speed C for each identified

wave, making use of a dispersion relation. However, Melville & Rapp (1988) remarked that the local maxima in dh/dt (or dh/dx) are ambiguous indicators of breaking. Instead, they suggested that surface velocity along the wave is a safer criterion, and must be used together with information on the surface elevation $h(t)$, or its temporal derivative, dh/dt.

The recent theoretical work of Longuet-Higgins (1985) is an example of several studies on vertical accelerations (d^2h/dt^2) in deep water waves. By considering progressive, irrotational, steep gravity waves of finite amplitude, Longuet-Higgins calculated an "apparent" vertical acceleration which was bounded by the value $0.22\,g$ on the positive side, but was unlimited in the direction of gravity, reaching exceedingly high negative values. On the other hand, the "real" or Lagrangian acceleration was found to vary between two limiting values, $0.30\,g$ and $-0.25\,g$. The above studies are also of interest to those studying waves in other geometries, mainly because they demonstrate the possible benefits and limitations of using surface displacement rates and accelerations.

From the viewpoint of data interpretation, presenting the rate of surface displacement dh/dt vs time does not seem to offer any advantages, compared to the $h(t)$ trace. However, the idea to replace time with film thickness and to plot $d\bar{h}/dt$ vs $\bar{h}$ appears to be very fruitful. Thus, a "spatial evolution portrait" of the film is obtained which contains much more information than the $h(t)$ and dh/dt traces separately and is particularly well-suited for identifying and studying roll waves, as will be discussed in this paper. Similarly, by plotting $d^2\bar{h}/dt^2$ vs $\bar{h}$ one can conveniently study Eulerian surface accelerations.

3. PRELIMINARY OBSERVATIONS

By simultaneously measuring the film thickness at two fixed stations, located along the main flow direction, one can examine the temporal and axial variation of the film surface. In our experimental apparatus (Karapantsios *et al.* 1989) the measuring probes were located 6 cm apart, approx. 2.5 m below the liquid film inlet.

By superposition of two simultaneously recorded traces (figure 1) one can obtain information on the development and the relative motion of various classes of waves. In general, all waves change to some extent from one measuring station to the other. The roll waves retain their identity and appear to travel with almost the same velocity. The shape of small waves (ripples) seems to change much more than that of roll waves. Moreover, it appears that (at least some) "bow" waves at the front of the roll waves move somewhat faster (5–20%), while those at the wave trough move somewhat slower, than the roll waves. It will be pointed out here that according to Chu & Dukler (1974) the celerity of small waves is much smaller than that of the roll waves. On the contrary, Maron *et al.* (1985) suggest that the small ("bow") waves, at the front of large waves, travel essentially with the same velocity.

Figure 2 shows an expanded in time film thickness trace and the corresponding variation of the time derivative dh/dt computed by finite differences. As expected, the maxima of dh/dt correspond to the front part of the waves.
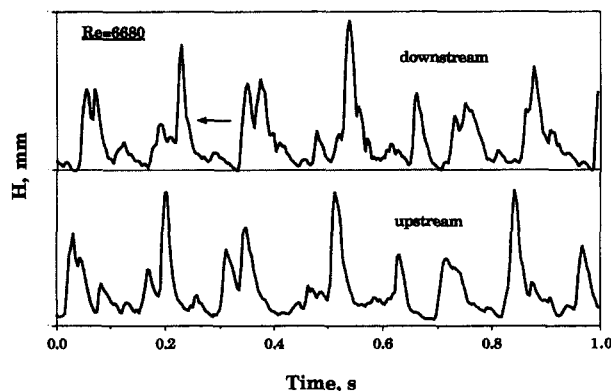

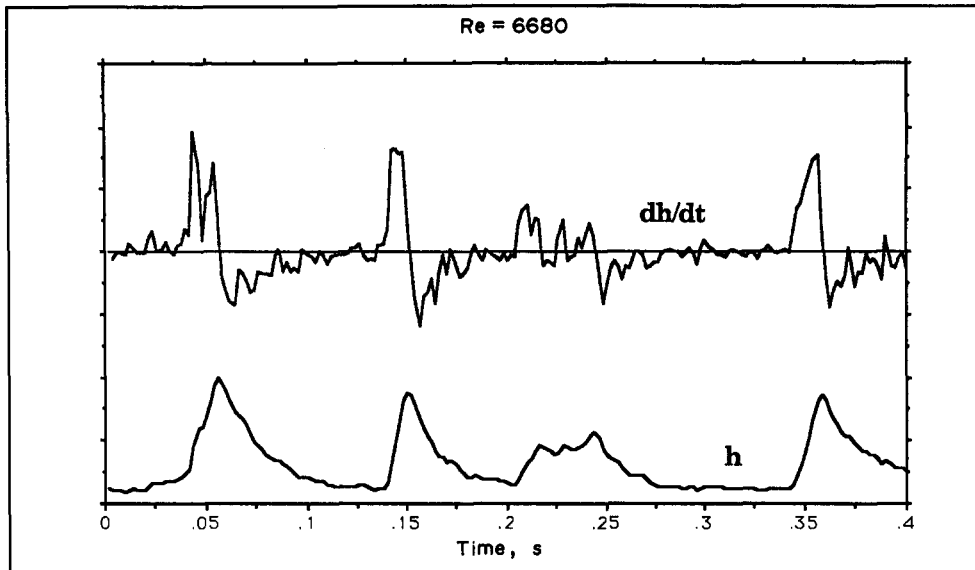Figure 1. Simultaneously recorded $h(t)$ traces at two locations, 6 cm apart in the axial direction.

Figure 2. A typical trace of the rate of displacement dh/dt with the corresponding film thickness trace $h(t)$.

Using time series data (Paras 1988) obtained at the two measuring stations the crosscorrelation functions of h and dh/dt are computed. The data set used here is comprised of 2048 points and was collected over a period of about 8 s for Re = 6680. The crosscorrelation functions (figure 3) show sharp peaks which coincide in the time domain. The measured phase lag of the upstream relative to the downstream measurement is $\tau = 0.028$ s. Therefore, since the distance between the probes is $l = 6$ cm, the average wave (phase) velocity is $C = l/\tau = 2.14$ m/s.

This value is smaller than the predictions given by Brauner (1987) for the turbulent regime $(U_w = 3.5$ m/s), greater than the average volumetric velocity $(U_v = 1.4$ m/s) and very close to the "Nusselt mean velocity" $(U_N = 2.1$ m/s). In fact, at high Re, literature data on wave phase velocities tend to approach the "Nusselt mean velocity". This is observed in the data by Chu (1973) and Zabaras (1985) as presented by Maron et al. (1985; their figure 4a), where it is further seen that for Re >4000 the wave phase velocity is the same for distances 1.94 and 4 m from the entry of the liquid film. Another interesting observation is the one made by Aragaki et al. (1987) who showed that for probe separation distances of 7 and 14 cm, the measured wave phase velocity is essentially the same. What makes this observation significant is the fact that their measurements were made within the so-called "undeveloped" flow region with the probes located approx. 1 m below the liquid inlet.
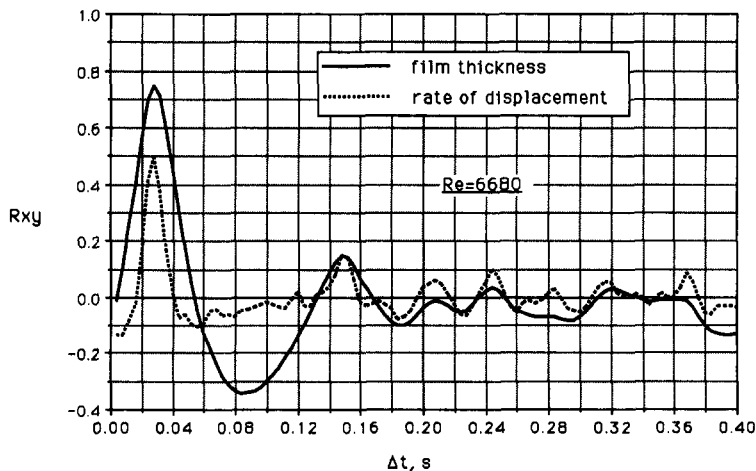

Figure 3. Crosscorrelation functions of film thickness and of the rate of displacement dh/dt [data by Paras (1988)].

The phase velocity of the time derivative dh/dt is the same as that of the roll waves (figure 3). However, the value of the crosscorrelation coefficient R_{xy} of the dh/dt time series is considerably smaller than that of film thickness, indicating a poorer correlation of the dh/dt data compared to the $h(t)$ data. Furthermore, the autocorrelation curve of the dh/dt time series (not shown here due to space limitations) exhibits the first zero crossing at a much shorter time interval than that in the corresponding $h(t)$ plot. This implies that the main features of the dh/dt signal retain their identity over a shorter time period compared to those of the $h(t)$ trace. Thus, the variation of dh/dt may provide a more stringent criterion for describing roll waves.

Plotting dh/dt vs h, as was discussed earlier, helps examine the spatial evolution of waves and verify the previously made comments. For comparison we present the "portraits" (figure 4) of a roll wave at two stations 6 cm apart along the vertical pipe. By inspecting the corresponding waves (marked with an arrow) in the film traces $h(t)$ of figure 1 one can hardly detect any change in the wave shape. Yet the plots in figure 4 appear to be more sensitive. For instance, the change in the wave slope at the trough of the downstream wave (exaggerated in the portrait in figure 4) is indicative of a small ripple which might evolve into a larger wave.

The plots in figure 4 clearly show that the rate dh/dt at both the front and back of a roll wave is not constant. Assuming that the wave celerity is constant, this remark is tantamount to saying that the surface slopes dh/dx are not constant either. It will be recalled here that in modeling efforts (e.g. Maron *et al.* 1985) the roll wave surface is assumed linear.

4. WAVE PROPERTIES

Figures 5(a, b) show typical data of the rate of displacement, dh/dt vs film height, h, for Re = 509 and 13090, respectively. The mean film thickness is also shown in these figures. Obviously, the high h values correspond to roll waves. Moreover, the extensive scatter in these graphs is representative of the roll waves for all Re.

It is evident that, for large (roll) waves, dh/dt covers a very large range of variation, i.e. between large positive and negative values. For the small waves this range is much smaller. The scatter is greater for positive than for negative dh/dt values. Indeed, it appears that the positive rate of displacement data correspond to absolute values roughly twice those of the negative dh/dt.

For small Re, large dh/dt values are observed only for waves which develop above the mean film thickness, i.e. roll waves. For large Re, relatively large time derivatives dh/dt appear also for small film thickness. This is indicative of another class of intermediate waves developing on the
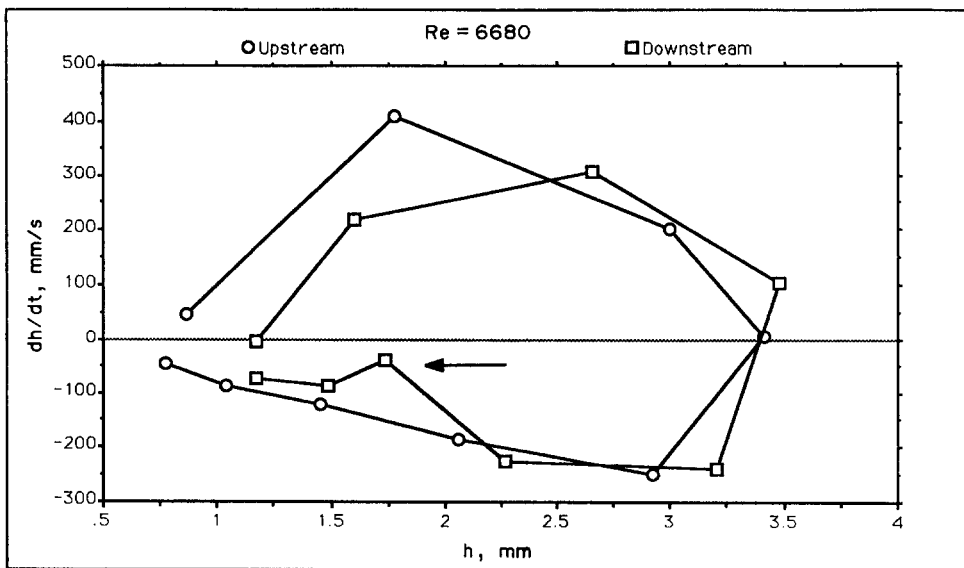

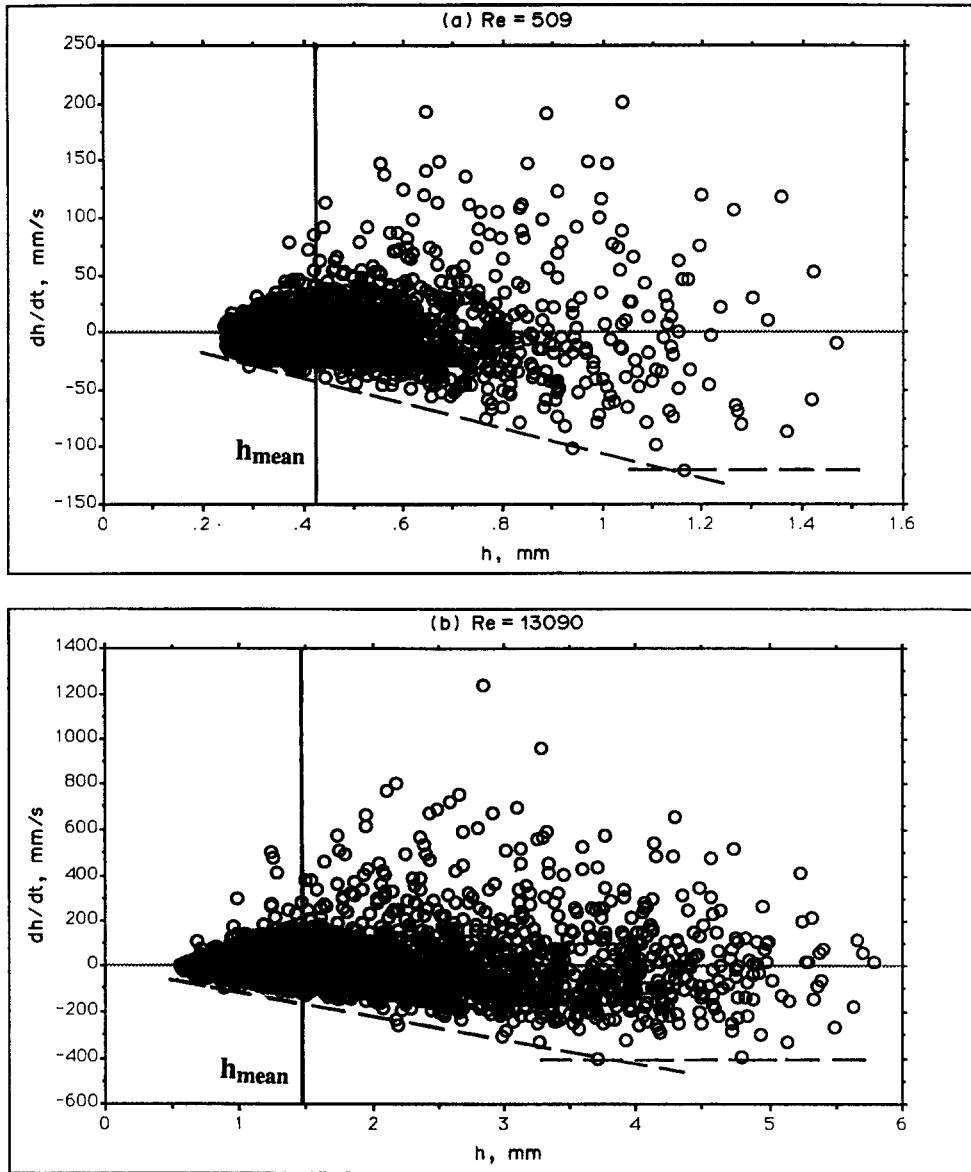Figure 4. Typical variation ("portrait") of the rate of displacement dh/dt with film thickness h for a roll wave.

Figure 5. Typical data of rate of displacement dh/dt vs film thickness h, for (a) small (Re = 509) and (b) large (Re = 13090) flow rates.

substrate, as was also concluded by statistically analyzing the film thickness traces (Karapantsios et al. 1989).

A common feature in all the data [figures 5(a, b)] concerns the negative dh/dt values. There is an envelope of these values (a line) which tends to decrease almost linearly with increasing h, down to a certain limiting value $(dh/dt)_{min}$ which remains nearly constant for large h, i.e. for the roll waves. These limiting values $(dh/dt)_{min}$ are presented in table 1 for various Reynolds numbers. Interestingly, $(dh/dt)_{min}$ is approx. constant (around -400 mm/s) for Re > 5000.

In table 1 the maximum dh/dt values, obtained from each data record, are also included. The corresponding range of values $[(dh/dt)_{max} - (dh/dt)_{min}]$ is plotted in figure 6 as a function of Re. An approximately linear variation is observed. These increasing values, however, are not necessarily associated with greater surface slopes, as will be shown in the next section.

In figures 7(a–d) (dh/dt) vs h data points are linked by straight-line segments. In each plot several roll waves can be easily identified. For clarity only a small data sample (750 data points) is used in these figures. It will be noticed that the temporal resolution of the measurements ($\Delta t = 0.002$ s)

Table 1. Approximate values of limiting rates of displacement for various Re

Re	$(dh/dt)_{max}$ (mm/s)	$(dh/dt)_{min}$ (mm/s)
509	201	−121
1114	374	−196
1720	342	−170
3535	518	−222
4745	561	−396
6680	570	−350
8949	1070	−470
9897	853	−383
13090	1235	−400
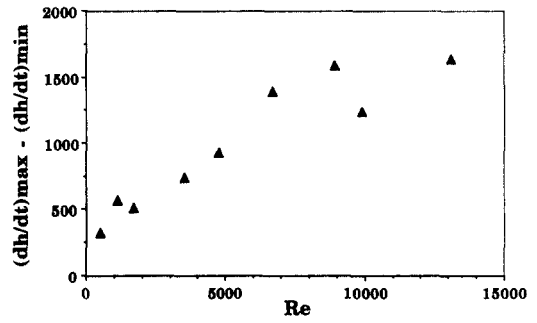
Figure 6. The influence of Re number on the range $[(dh/dt)_{max}-(dh/dt)_{min}]$ of time derivatives.
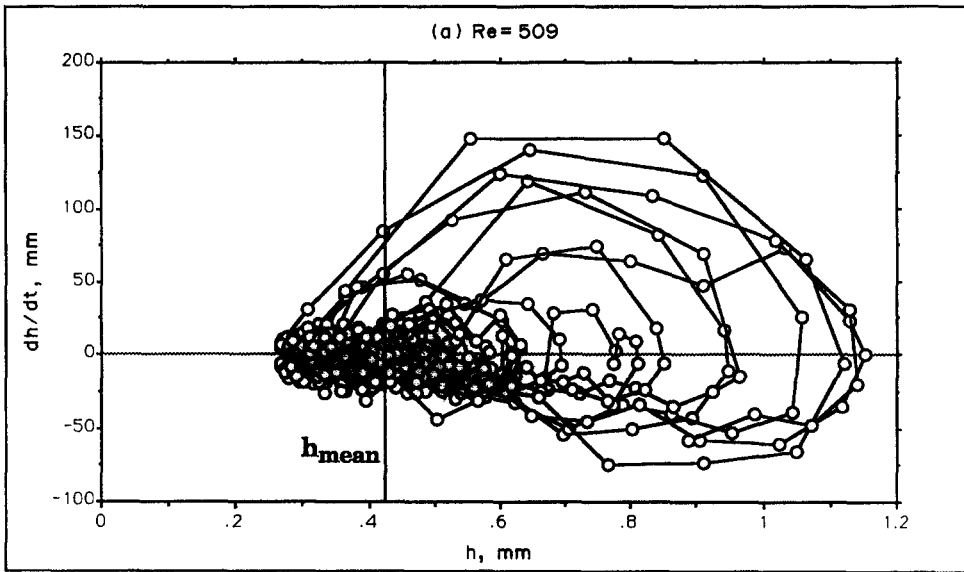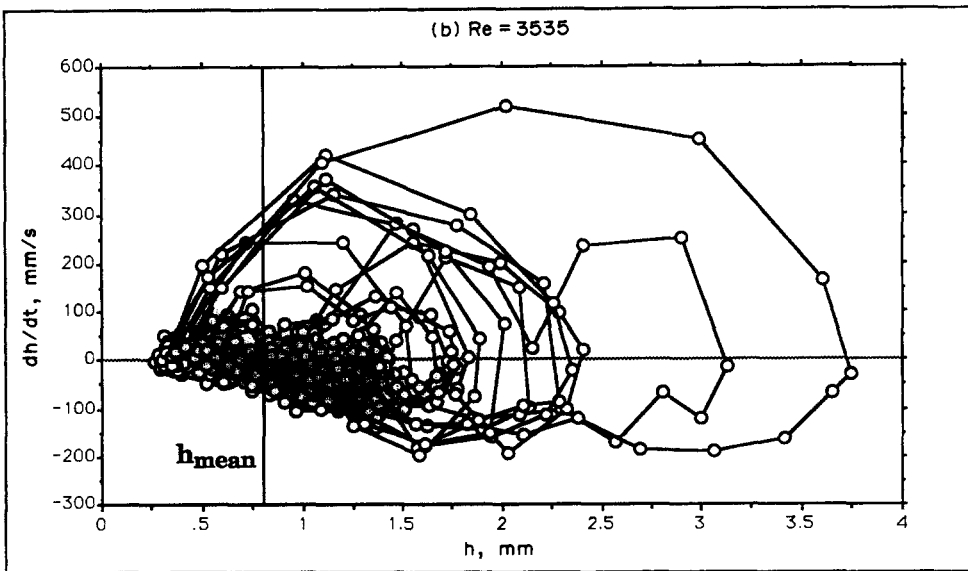

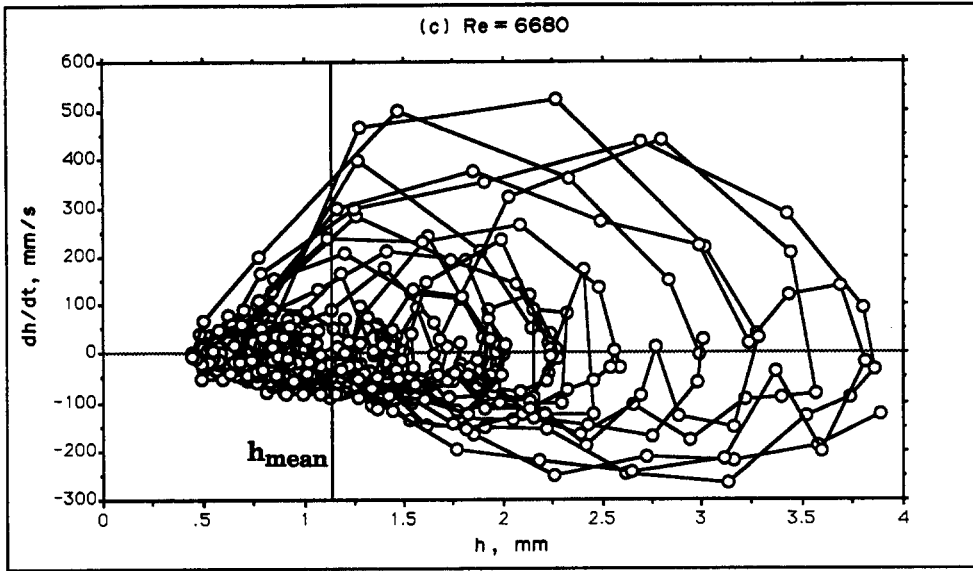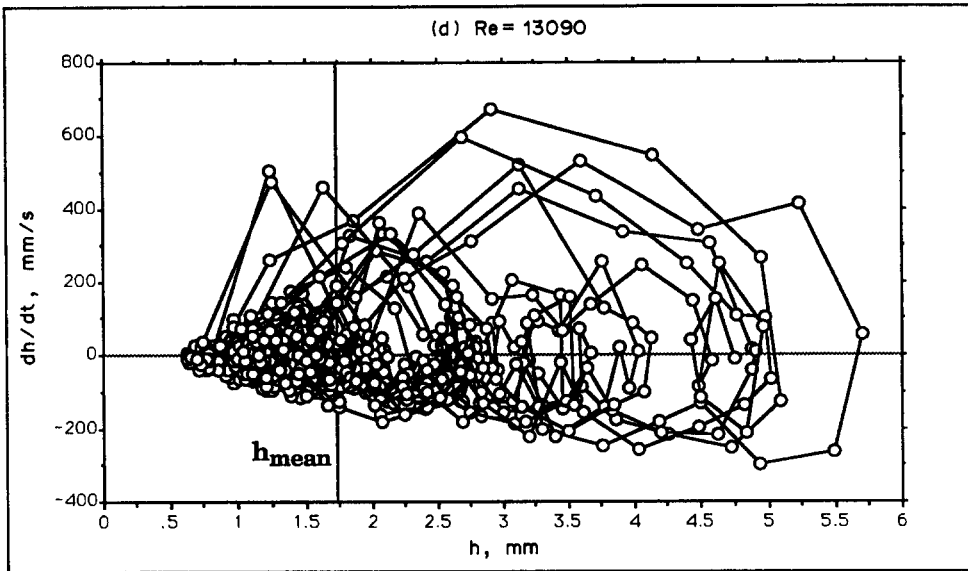Figure 7(a)

Figure 7(b)

Figure 7(c)

Figure 7(d)

Figure 7. Typical plots of dh/dt vs h data for various Re.

does not permit the accurate depiction of small waves (ripples), most of which appear to be described by less than five data points.

All roll waves have a very similar form, especially those recorded at the same Re. In fact, the Re value does not appear to influence significantly the form of roll waves. The curves representing this "spatial evolution portrait" have a shell-like shape. Initially, as the wave emerges from the substrate, the rate dh/dt seems to increase almost linearly with h up to a maximum value, whereafter it tends to decrease towards negative values following a convex curve. It is also noted that the maximum dh/dt of *each* roll wave occurs at its front, at a level (h) well above the mean film thickness h_{mean}. Near the wave peak large changes of dh/dt are observed, while at the wave back, as expected, the rate of displacement becomes negative.

The similarity of the dh/dt portraits of roll waves suggests further examination of their characteristics. In order to study the range of dh/dt variation, the ratio of $(dh/dt)_{max}$ and $(dh/dt)_{min}$

values of *individual* waves was computed. Extensive calculations carried out on the data of Karapantsios *et al.* (1989) showed that for Re < 5000,

$$1.5 < \left| \frac{\left(\dfrac{dh}{dt}\right)_{max}}{\left(\dfrac{dh}{dt}\right)_{min}} \right| < 3.0, \tag{7}$$

and for 5000 < Re < 13000,

$$1.5 < \left| \frac{\left(\dfrac{dh}{dt}\right)_{max}}{\left(\dfrac{dh}{dt}\right)_{min}} \right| < 4.0. \tag{8}$$

The broadening of this range at high Re is in line with the conclusion of Karapantsios *et al.* (1989) that above Re $\approx$ 5000 a change in the flow apparently occurs. Indeed, the data of that study (their figures 5 and 7) show that above Re $\approx$ 5000 the amplitude of roll waves does not significantly increase with increasing Re, the increasing flow rate being accommodated by the increase of the *substrate* thickness.

Careful inspection of the portraits in figures 7(a–d) reveals another interesting feature. The h_{peak} of the roll waves seems to be related to the initial slope $\Delta(dh/dt)/\Delta h$. In particular, the higher waves (large h) usually correspond to lower $\Delta(dh/dt)/\Delta h$ values, while small waves (ripples) appear to exhibit substantially larger slopes. For Re < 5000, the distinction between large and small waves, in terms of the $\Delta(dh/dt)/\Delta h$ slope, is rather easy. However, for Re > 5000 a new type of wave appears, with amplitude clearly in between those of the large and the small waves. They are "intermediate" waves with a peak height (h_{peak}) definitely larger than the mean film thickness, so they are not to be confused with the small waves. Typically, they emerge from small h (below h_{mean}) with $\Delta(dh/dt)/\Delta h$ slopes much larger than the slopes of the large waves. Such "intermediate" waves are clearly seen in figure 7(d), for Re = 13090, but they are completely absent in figure 7(a), for Re = 509.

The possibility of relating the rate of change $B \equiv \Delta(dh/dt)/\Delta h$ to surface fluctuations is demonstrated in figure 8, where the film thickness and the corresponding B trace are presented. The $h(t)$ scale in this figure is arbitrary. It is interesting that the fluctuating B values corresponding to ripples on the substrate are significantly larger than those of the roll waves. Thus, one is tempted to argue that this quantity (B) is a sensitive criterion for characterizing rippled interfaces, and for
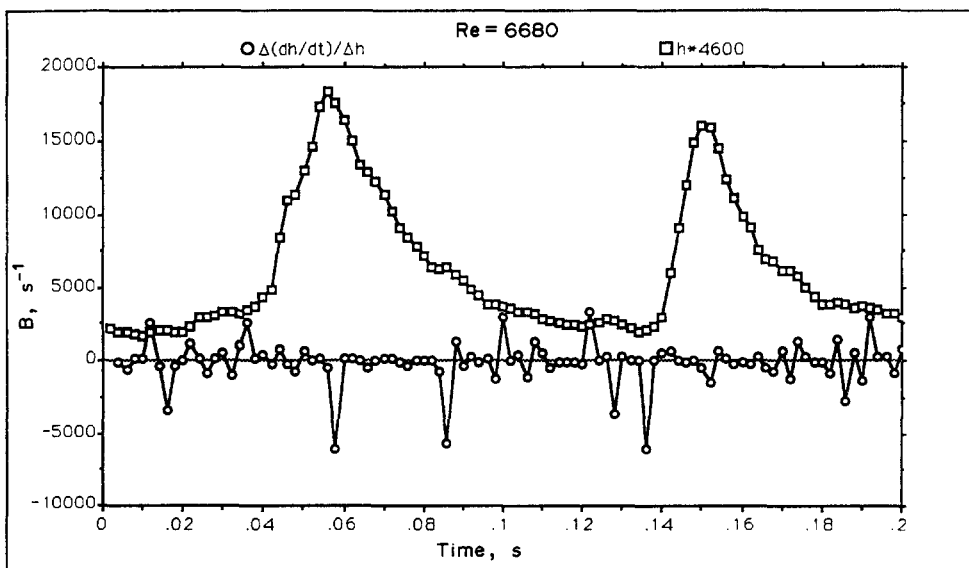

Figure 8. Traces of film thickness and of the corresponding rate of change $B \equiv \Delta(dh/dt)/\Delta h$, for Re = 6680.
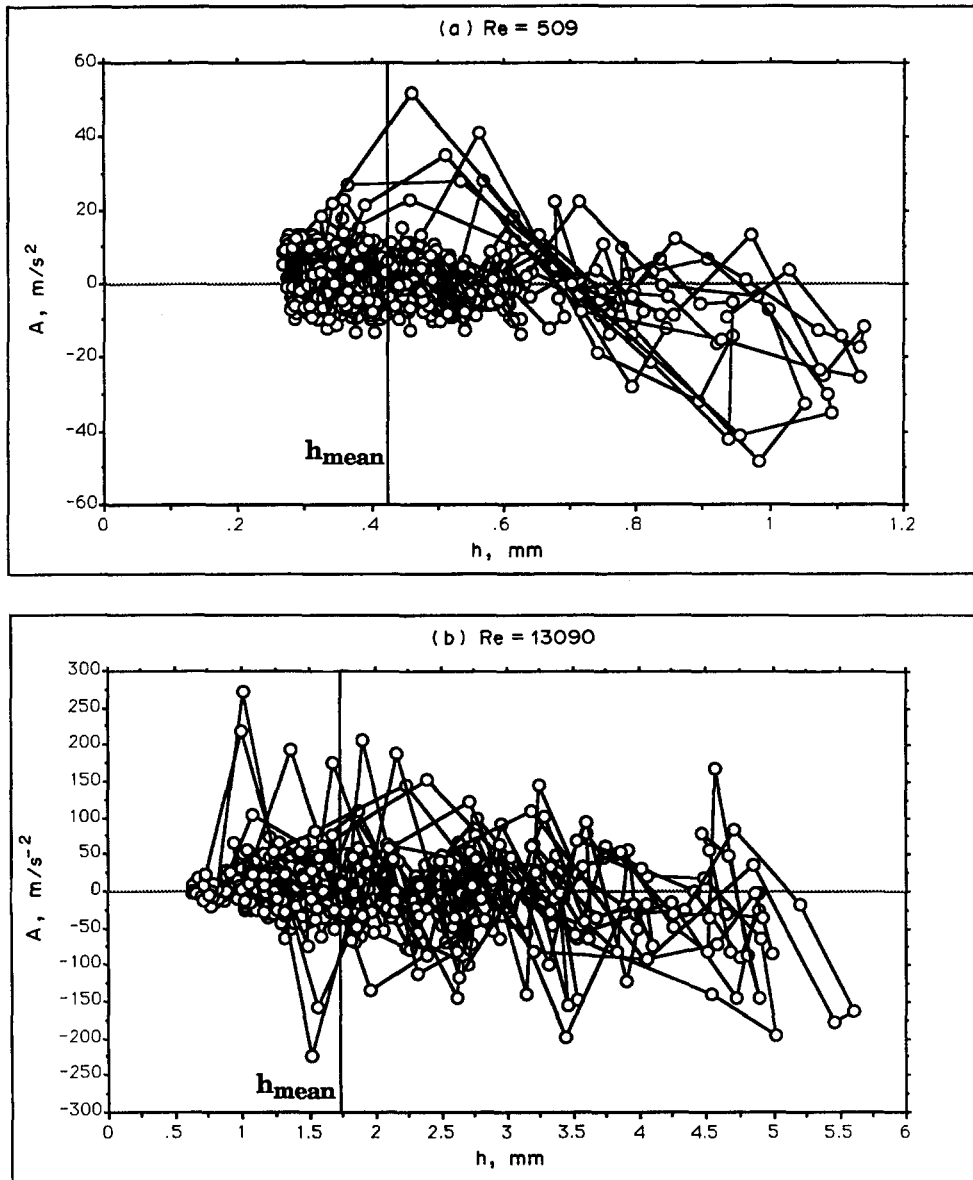
Figure 9. "Apparent" surface accelerations $A = d^2h/dt^2$ vs film thickness for (a) Re $= 509$ and (b) Re $= 13090$.

detecting ripples deemed insignificant in usual $h(t)$ time series statistical analysis. However, one should withhold judgment on the value of this quantity until questions relating to the frequency of data acquisition and to the overall accuracy (response, resolution etc.) of the experimental technique are resolved.

In figures 9(a, b) the quantity $d^2h/dt^2 \approx \Delta(dh/dt)/\Delta t \equiv A$, discussed in section 2, is plotted against the thickness h. This quantity represents the "apparent" (Eulerian) local acceleration (positive values) and deceleration (negative values) of the surface. At first glance, the values of d^2h/dt^2 are surprisingly high (up to 30 times the acceleration of gravity, g) especially at high Re. It is easy, however, to account for such large values by recalling that d^2h/dt^2 is directly related with the local radius of curvature (R) of the liquid surface. Indeed, it can be shown that for permanent waves

$$\frac{1}{R} = \frac{\partial^2 h}{\partial x^2} = \frac{1}{C^2}\frac{\partial^2 h}{\partial t^2}.$$ [9]

For large Re, typical values for roll waves are $C^2 = O(10)$ and $(d^2h/dt^2) = O(100)$, so that $R = 10$ cm. This is quite a reasonable radius of curvature for the waves of long wavelength studied

here. Moreover, it is of interest to recall the work of Longuet-Higgins (1985) who reported that the "apparent" accelerations of steep gravity waves, at the wave crest, can take very large (in fact infinite) negative values.

In our data, the absolute values of positive and of negative d^2h/dt^2 are nearly equal. The highest positive d^2h/dt^2 values are observed at the substrate ($h < h_{mean}$), while the highest negative values are mostly above the h_{mean} and around the wave peaks. This description applies better to low and moderate Re, while at higher Re the data tend to be uniformly scattered about the h axis.

5. STATISTICAL CHARACTERISTICS

Additional useful information can be obtained by statistically analyzing the data on time derivatives of the surface elevation. The definition of statistical quantities employed in this section has been given in Karapantsios et al. (1989).

Figure 10(a) shows the probability density distribution (PDD) of dh/dt at Re = 509. Clearly this distribution is not Gaussian. The shapes of the PDD at other Re values also deviate from the normal distribution, as shown in figure 10(b) for Re = 13090. This deviation is quantified in
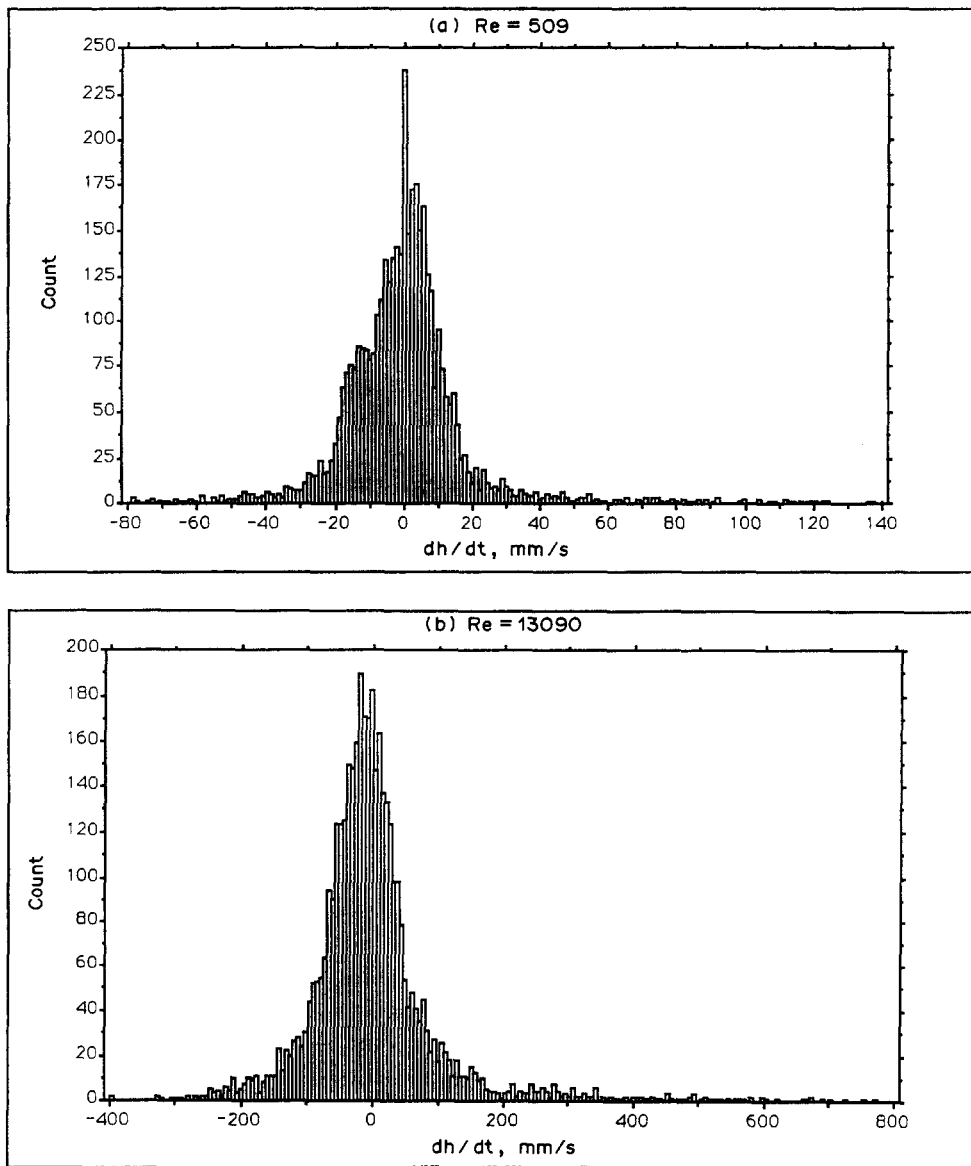

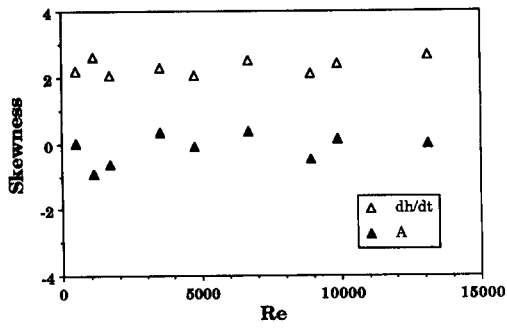Figure 10. PDD of rates of surface displacement for (a) Re = 509 and (b) Re = 13090.

Figure 11. The coefficient of skewness (a_3) of time derivatives dh/dt and $A = d^2h/dt^2$ for various Re.
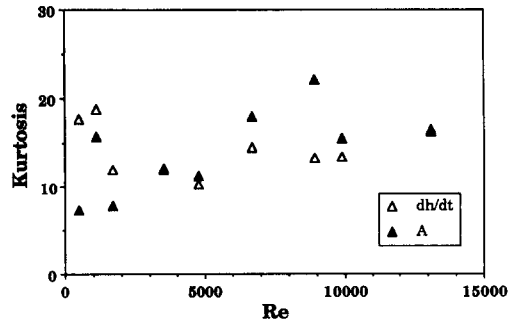
Figure 12. The coefficient of kurtosis (a_4) of time derivatives dh/dt and $A = d^2h/dt^2$ for various Re.

figures 11 and 12 where the coefficient of skewness (a_3) and the coefficient of kurtosis (a_4) are plotted, respectively. It will be recalled that for a Gaussian distribution $a_3 = 0$ and $a_4 = 3$. The distribution of the (dh/dt) time series is slightly skewed to the right $(a_3 \approx 2.0–2.7)$ throughout the Re range studied. For the film thickness time series the calculated skewness is $a_3 \approx 1.5–3.0$. The distribution (PDD) of $A = d^2h/dt^2$ is more symmetric, with a_3 values quite close to zero.

The coefficient of kurtosis is considerably larger than the value $a_4 = 3$ corresponding to Gaussian distributions. Figure 12 shows that both derivatives have kurtosis values varying between 10 and 20 throughout the Re range of the measurements. The coefficient of kurtosis for the film thickness time series $h(t)$ is between 2.5 and 12 (Karapantsios et al. 1989), i.e. much smaller.

It is interesting to note that in the case of wind-induced sea waves the skewness of the surface slopes dh/dx (which is equivalent to dh/dt) is quite small, i.e. of order one (Longuet-Higgins 1982). A theoretical explanation, which leads to correct predictions in magnitude and sign, is that the slope skewness is caused by short ripples (or capillary–gravity waves) being modulated by the presence of the long waves on which they ride (Longuet-Higgins 1982). Obviously, a different mechanism is causing the larger skewness of surface slopes on falling films and care must be exercised when making comparisons.

By sorting in descending order the entire set of 4000 dh/dt data points (for each Re) some interesting results are obtained. All data sets show that the *negative* values are approx. 2400, i.e. $(2400/4000) = 60\%$ of the population, while the remaining 40% are *positive*. Using a simplified conservation equation in the horizontal direction (perpendicular to the main flow direction)one obtains

$$(60\% \text{ data points}) \left| \text{negative} \frac{dh}{dt} \right| - (40\% \text{ data points}) \left| \text{positive} \frac{dh}{dt} \right| = 0,$$

where representative negative and positive rates are used. Then

$$\frac{\left| \text{positive} \dfrac{dh}{dt} \right|}{\left| \text{negative} \dfrac{dh}{dt} \right|} = 1.5. \tag{10}$$

It will be stressed that this result is deduced from the entire set of data points, not just the roll waves. On the other hand, by examining *individual* waves, it was observed in the previous section that

$$1.5 < \left| \frac{\left(\dfrac{dh}{dt} \right)_{max}}{\left(\dfrac{dh}{dt} \right)_{min}} \right| < 3 \text{ or } 4, \tag{11}$$

depending on the range of Re. One may, therefore, conclude that throughout the Re range studied, $(dh/dt)_{max}/(dh/dt)_{min} = 1.5$ is a *lower bound* for the ratio of positive to negative rates of displacement for all kinds of waves; small, intermediate or large. This lower bound may be considered a hydrodynamic characteristic of the system.
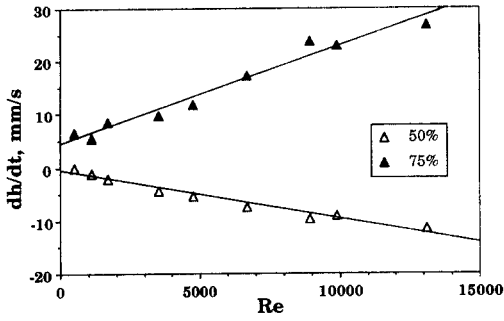
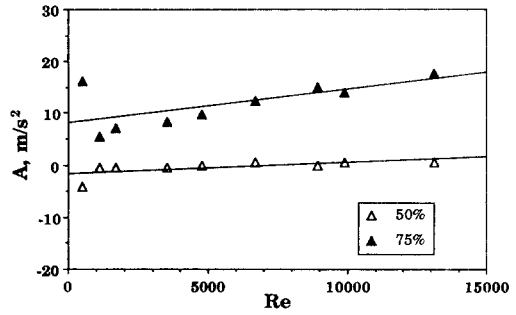Figure 13. The influence of Re on the points corresponding to 50 and 75% of the population of dh/dt.

Figure 14. The influence of Re on the points corresponding to 50 and 75% of the population of $A = d^2h/dt^2$.

Interesting observations are also made by plotting the dh/dt value of the No. 2000 data point (50% of the set) and the No. 3000 data point (corresponding to 75%) against Re. Figure 13 shows that an almost perfect linearity is obtained.

Analyzing the d^2h/dt^2 data in the same fashion (figure 14) does not lead to correlations as good as those of dh/dt . It is worth pointing out, however, that the "50% data point" is approx. 0 for all Re. This is another indication of the quite symmetrical PDD of d^2h/dt^2.

As was pointed out in the Introduction, the waviness of the air/liquid interface is considered responsible for the enhancement of transport processes. We shall, therefore, attempt to estimate the fraction of the surface which remains undisturbed (flat or nearly flat) during the flow. It can be argued that the measuring technique employed by Karapantsios et al. (1989) can resolve height differences of at least 2 μm. Taking into account the temporal resolution, due to sampling frequency (500 Hz), $\Delta t = 2$ ms, it is estimated that the smallest detectable rate of displacement in their experimental setup is 1 mm/s. Thus, all dh/dt values equal to, or smaller than, 1 mm/s are considered "zero". Plotting the fraction of these "zero" rates vs Re shows an almost perfect exponential reduction (figure 15).

Although the aforementioned criterion may be somewhat conservative, it provides a measure of the influence of Re on the rate of surface displacement and on film waviness. Assuming that the criterion is realistic, it is noted that the fraction of nearly flat surface is small even for the smallest measured Re.

Another important piece of information which is obtained from the rate of displacement data is the range of variation of surface slopes as a function of Re. Making use of [1] along with the data on (dh/dt)$_{max}$ and (dh/dt)$_{min}$ the maximum and minimum surface slopes are computed. Figure 16 shows the calculated slopes in degrees. The necessary wave phase velocities were obtained by interpolation from Zabaras' (1985) thesis for Re < 5000, and one value at Re = 6680 was taken by Paras (1988). For Re > 7000, the "Nusselt mean velocity" was employed, as it seems to roughly coincide with the phase velocity at such high Re (Maron et al. 1985; Aragaki et al. 1987).

The results plotted in figure 16 are remarkable. Throughout the Re range examined, the maximum (wave front) and the minimum (wave back) slopes appear to be almost constant, with only one exception at Re = 1720. The maximum slopes may increase very weakly with Re, being
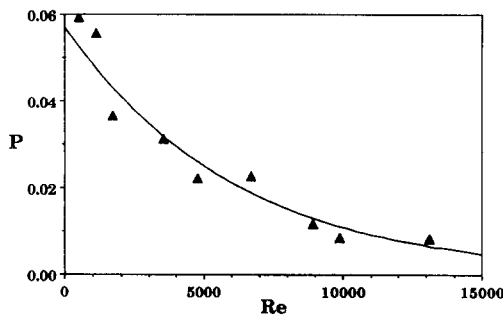

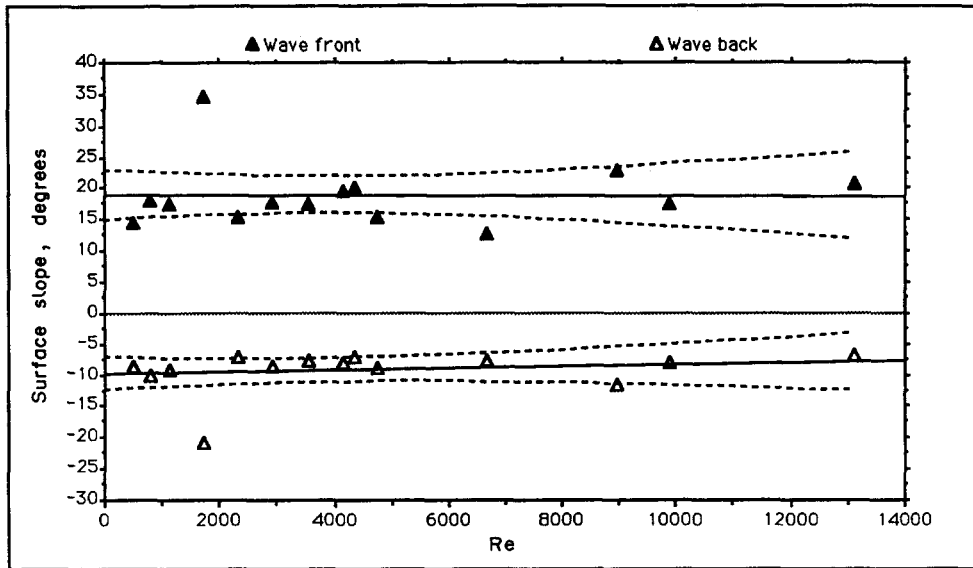Figure 15. The fraction of "undisturbed" film surface as a function of Re.

Figure 16. Estimated maximum and minimum wave slopes for Re = 509 to 13090.

scattered in the range $14°–23°$. The minimum slopes vary randomly between $-7°$ and $-11.5°$, showing no dependence on Re. The dotted lines in figure 16 mark the confidence interval in the predictions of the regression line (95% confident mean value).

This narrow and nearly constant range of surface slopes is considered a significant feature of the falling films. It will be recalled here that Alekseenko *et al.* (1985), studying strictly two-dimensional waves, computed maximum surface slopes of approx. $23°$ at Re $\ll 50$. Furthermore, the maximum surface slope of a regular progressive ocean wave is approx. $30°$, as calculated by Longuet-Higgins & Fox (1977).

6. DISCUSSION OF RESULTS

By plotting data on time derivatives dh/dt and d^2h/dt^2 against the corresponding film thickness h, it is possible to extract more information about wavy surfaces than a usual statistical analysis of $h(t)$ can offer. The plot of dh/dt against h contains in a condensed form a great deal of useful information. Of particular interest is the "spatial evolution portrait" of roll waves obtained in this type of plot, showing their characteristic features, such as the variation of surface slopes in their front and their back and the peak height. Despite the sensitivity of this plot to very small surface fluctuations, the similarity of portraits of all the roll waves in a record (for Re constant) is evident. A shell-like pattern of roll wave evolution is easily recognized. More significant, perhaps from the point of view of modeling, is the close similarity of typical portraits for various Re. Indeed, this type of plot may facilitate the development of generalized analytical expressions for describing roll wave shapes.

The magnitude of positive rates of displacement is greater than that of the negative rates. The ratio $(dh/dt)_{max}/(dh/dt)_{min}$ examined in individual waves and in the entire data sample shows a lower bound of 1.5 throughout the Re range and an upper bound of 3.0–4.0 depending on Re. It is interesting that the $(dh/dt)_{min}$ of all the data above Re ≈ 5000 is nearly constant at about -400 mm/s, whereas $(dh/dt)_{max}$ increase linearly with Re, throughout the Re range. The $(dh/dt)_{min}$ (i.e. maximum negative slopes) correspond to the back of roll waves. Other relevant statistical quantities, such as the 50 and 75% points of the dh/dt data record, also show a linear increase with Re.

The maximum and minimum wave surface slopes obtained for the range Re ≈ 500 to 13000 show a remarkable lack of dependence on flow rate. One might attempt to explain this result for the minimum slopes (back of roll waves) on the basis of the flow recirculation region proposed by Maron *et al.* (1985), by assuming that the inertia of the reverse flow does not allow negative slopes

greater than a certain value. No explanation can be offered at this time for the lack of Re dependence of maximum slopes, usually observed at the wave front.

The quantity $B \equiv \Delta(\mathrm{d}h/\mathrm{d}t)/\Delta h$—a slope in the $\mathrm{d}h/\mathrm{d}t$ vs h plots—is useful in studying the evolution of a wave and in distinguishing various types of waves, e.g. gradually developing roll waves or sharply emerging waves from the substrate. It is also proposed here to explore in future studies the possible use of this quantity (B) as a criterion for characterizing rippled interfaces, due to the high sensitivity of B to slight surface perturbations.

Using the smallest detectable rate of displacement (of our experimental setup) as a criterion, the fraction of the undisturbed film surface was found to be small (≈ 0.06 at Re $= 509$), decreasing almost exponentially with Re.

The data on Eulerian surface acceleration can be used to develop a physical explanation for some aspects of film flow. For falling films, as is well-known, *inertia* is a destabilizing force, whereas viscous stresses and interfacial tension have a "restoring" influence. The significance of surface tension forces can be examined by using the so-called Bond number,

$$\mathrm{Bo} = \frac{(\rho_\mathrm{L} - \rho_\mathrm{G})gR^2}{\sigma} ,$$ [12]

which represents the ratio of gravitational to surface forces. Here R is one of the principal radii of curvature of the free surface, given by [9]. For interfacial tension forces to be significant, compared to gravitational forces, Bo must be of order 1. For water one obtains

$$\mathrm{Bo} = 13.63C^4 \left(\frac{\mathrm{d}^2 h}{\mathrm{d}t^2}\right)^{-2} ,$$

which shows that the apparent acceleration must take high values, corresponding to *small* surface curvature, in order to have significant surface tension effects. Substituting typical values of C (Zabaras 1985) and the corresponding values of $\mathrm{d}^2 h/\mathrm{d}t^2$ obtained here [figures 9(a, b)], one finds that Bo is almost always much larger than unity in the Re range of our data. Only at low Re (e.g. Re = 509) are values close to unity obtained. It is clear, therefore, that interfacial tension forces only act as a restoring force in the case of small ripples (at relatively small Re) which are characterized by small curvature or large apparent acceleration $\mathrm{d}^2 h/\mathrm{d}t^2$.

It is of interest to point out in our data that at *small* Re [figure 9(a)] and above a certain film thickness h, essentially only *negative* $\mathrm{d}^2 h/\mathrm{d}t^2$ values are obtained, even at points where the surface slope is positive. Thus, for *relatively small Re*, a fairly well-organized roll wave motion is observed with an accelerating front and a decelerating region, covering the crest and part of the back of the wave. At *large Re* [figure 9(b)] the picture is quite different. The surface accelerations and decelerations are almost evenly distributed about the $A = 0$ axis, with high negative $\mathrm{d}^2 h/\mathrm{d}t^2$ values also observed below h_mean, i.e. at the substrate. Other plots similar to those of figures 9(a, b) show that this (more random) wavy flow, with more frequently accelerating–decelerating surface regions, is evident above Re ≈ 5000. This is in agreement with the observations made in a previous paper (Karapantsios *et al.* 1989), i.e. that above Re ≈ 5000 there is gradual amplification of ripples into intermediate waves in the substrate. Apparently, these waves with the significant accelerations–decelerations can dissipate some of the increased potential energy at the higher flow rates.

On the basis of all the evidence obtained in our work the following possible physical picture emerges:

At relatively low Re the substrate is very thin and the ripples on its surface are damped mainly by viscous stresses and to some extent by capillary pressure. At relatively high Re (above Re ≈ 5000) the thickness of the substrate tends to increase with Re. The small waves on the substrate surface tend to grow while the roll wave amplification tends to decrease drastically. Additionally, the shape of the roll waves does not change significantly and their phase velocity tends to a value, nearly equal to Nusselt velocity. It is likely that at these higher Re the thick substrate, accommodating a large portion of the flowing liquid, acts at the same time as a dampener inhibiting the growth of roll waves.

The results obtained in this work are tacitly attributed to a well-developed wave structure, although they are based only on data taken at a distance $x = 2.5$ m from the liquid entry point. No measurements were made to prove that at this distance the flow is indeed well-developed. However, there is experimental evidence in the literature suggesting that data taken at 2.5 m may be considered representative of conditions close to an equilibrium wave structure. Most of the statistical parameters obtained by Takahama & Kato (1980) at $x = 1.74$ m, as well as the wave celerities at high Re measured by Zabaras (1985) at $x = 1.97$ m and Chu & Dukler (1975) at $x = 4.3$ m support this claim. More work is certainly required to clarify this issue and to establish the influence of various factors on the length required to reach fully-developed conditions. It must be added though that this may not be an easy task. In fact, preliminary measurements in our laboratory indicate that the development of a wave structure is influenced, in addition to fluid mechanical factors, by the dynamic stability of the entire equipment (pipe with supports).

Another point of concern is the accuracy of the experimental technique ("parallel wires") used in this study. This technique is considered superior to others, especially for measurements of film thickness variation with time. However, it has obvious limitations, with regard to spatial resolution and frequency response, due to the two wires and to possible meniscus/liquid drainage effects. Additionally, as is pointed out in section 4 of this paper, the sampling frequency employed (500 Hz) may not permit the detection of *very small waves*. Despite these limitations, the main results of this work concerning roll waves with a characteristic frequency of order 10 Hz are correct and they are not expected to be altered by a higher sampling frequency. However, in order to examine the frequency response of the technique and to improve the temporal resolution of the measurements, our data acquisition system has been upgraded to make measurements with much higher sampling frequencies.

REFERENCES

ALEKSEENKO, S. V., NAKORYAKOV, V. E. & POKUSAEV, B. G. 1985 Wave formation on vertical falling liquid films. *Int. J. Multiphase Flow* **11**, 607–627.

ARAGAKI, T., NAKAYAMA, S., SUZUKI, M. & TOYAMA, S. 1987 Characteristics of a falling film on a vertical tube. *Int. chem. Engng* **27**, 326–333.

BACH, P. & VILLADSEN, J. 1984 Simulation of the vertical flow of a thin wavy film using a finite-element method. *Int. J. Heat Mass Transfer* **27**, 815–827.

BACK, D. D. & MCCREADY, M. J. 1988 Theoretical study of interfacial transport in gas–liquid flows. *AIChE Jl* **34**, 1789–1802.

BENJAMIN, T. B. 1957 Wave formation in laminar flow down an inclined plane. *J. Fluid Mech.* **2**, 554–574.

BENNEY, D. J. 1966 Long waves in liquid film. *J. math. Phys.* **45**, 150–155.

BRAUNER, N. 1987 Roll wave celerity and average film thickness in turbulent wavy film flow. *Chem. Engng Sci.* **42**, 265–273.

BRAUNER, N. & MARON, D. M. 1982 Characteristics of inclined thin films, waviness and the associated mass transfer. *Int. J. Heat Mass Transfer* **25**, 99–110.

CHANG, H. C. 1987 Evolution of nonlinear waves on vertically falling films—a normal form analysis. *Chem. Engng Sci.* **42**, 515–533.

CHU, K. J. 1973 Statistical characterization and modelling of wavy liquid films in vertical two-phase flow. Ph.D. Thesis in Chemical Engineering, Univ. of Houston, Tex.

CHU, K. J. & DUKLER, A. E. 1974 Statistical characteristics of thin, wavy films, Part II. Studies of the substrate and its wave structure. *AIChE Jl* **20**, 695–706.

CHU, K. J. & DUKLER, A. E. 1975 Statistical characteristics of thin, wavy films, Part III. Structure of the large waves and their resistance to gas flow. *AIChE Jl* **21**, 583–593.

GLAZMAN, R. E. 1986 Statistical characterization of sea surface geometry for a wave slope field discontinuous in the mean square. *J. geophys. Res.* **91**, 6629–6641.

HENSTOCK, W. H. & HANRATTY, T. J. 1979 Gas absorption by a liquid layer flowing on the wall of a pipe. *AIChE Jl* **25**, 122–131.

KAPITSA, P. L. 1964 Wave flow of thin layers of a viscous fluid. In *Collected Papers of P. L. Kapitsa*. Macmillan, New York.

KARAPANTSIOS, T. D., PARAS, S. V. & KARABELAS, A. J. 1989 Statistical characteristics of free falling films at high Reynolds numbers. *Int. J. Multiphase Flow* **15**, 1–21.

KHESHGI, H. S. & SCRIVEN, L. E. 1987 Disturbed film flow on a vertical plate. *Phys. Fluids* **30**, 990–997.

LIN, S. P. 1974 Finite amplitude side-band stability of a viscous film. *J. Fluid Mech.* **63**, 417–429.

LONGUET-HIGGINS, M. S. 1982 On the skewness of sea-surface slopes. *J. phys. Oceanogr.* **12**, 1283–1291.

LONGUET-HIGGINS, M. S. 1985 Accelerations in steep gravity waves. *J. phys. Oceanogr.* **15**, 1570–1579.

LONGUET-HIGGINS, M. S. & FOX, M. H. 1977 Theory of the almost-highest wave: the inner solution. *J. Fluid Mech.* **80**, 721–741.

LONGUET-HIGGINS, M. S. & SMITH, N. O. 1983 Measurement of breaking waves by a surface jump meter. *J. geophys. Res.* **88**, 9823–9831.

MARON, D. M., BRAUNER, N. & DUKLER, A. 1985 Interfacial structure of thin falling films: piecewise modelling of the waves. *Physicochem. Hydrodynam.* **6**, 87–113.

McCREADY, M. J. & HANRATTY, T. J. 1985 Effect of air shear on gas absorption by a liquid film. *AIChE Jl* **31**, 2066–2074.

MELVILLE, W. K. & RAPP, R. J. 1988 The surface velocity field in steep and breaking waves. *J. Fluid Mech.* **189**, 1–22.

NAKAYA, C. 1975 Long waves on a thin fluid layer flowing down an inclined plane. *Phys. Fluids* **18**, 1407–1412.

PARAS, S. V. 1988 Unpublished data. Dept of Chemical Engng, Univ. of Thessaloniki, Greece.

PUMIR, A., MANNEVILLE, P. & POMEAU, Y. 1983 On solitary waves running down an inclined plane. *J. Fluid Mech.* **135**, 27–50.

TAKAHAMA, H. & KATO, S. 1980 Longitudinal flow characteristics of vertically falling liquid films without concurrent gas flow. *Int. J. Multiphase Flow* **6**, 203–215.

THORPE, S. A. & HUMPHRIES, P. N. 1980 Bubbles and breaking waves. *Nature* **283**, 463–465.

WASDEN, F. K. & DUKLER, A. E. 1989 Insights into the hydrodynamics of free falling films. *AIChE Jl* **35**, 187–196.

XU, D., HWANG, P. A. & WU, J. 1986 Breaking of wind-generated waves. *J. phys. Oceanogr.* **16**, 2172–2178.

ZABARAS, G. J. 1985 Studies of vertical annular gas–liquid flows. Ph.D. Thesis in Chemical Engineering, Univ. of Houston, Tex.